Lawrence Livermore National Laboratory

LLYMP9708036 QA: N
August 8, 1997

Larry Hayes, Manager
Scientific Program Operations
CRWMS Management & Operations Contractor
1180 Town Center Drive
Las Vegas, NV 89134

ATTN: Terry Grant

SUBJECT: Completion of Level 4 Milestones: SPLC2M4 and SPLC3M4 (TR3C1FB5) Reports: Distribution of Post-Emplacement Seepage into the Repository Drifts with Parametric Variation of Intrinsic Properties and Models and Bounds for Post-Emplacement Seepage into the Repository(WBS 1.2.3.12.2)

Enclosed are the subject milestones, which have a due date of 7/31/97. These deliverables meet the criteria as described in the LLNL SOW. The two deliverables have been combined into one report.

If you have questions, contact John Nitao at (510) 423-0297.

Dale G. Wilder
TAL for Near Field Environment Characterization

DGW/BB/bb

Enclosure

Distribution of Post-Emplacement Seepage into the Repostory Drifts with Parametric Variation of Intrinsic Properties

Milestone Level 4
Deliverable No. SPLC2M4

Models and Bounds for Post-Emplacement Seepage into the Repository

Milestone Level 4
Deliverable No. SPLC3M4

John J. Nitao
L-206
Lawrence Livermore National Laboratory
Livermore, CA, 94551

1. Objective

Preliminary calculations of seepage into drifts under isothermal conditions (Nitao, 1996) are relevant primarily for the post-thermal period after the effects of radioactive waste heat from waste packages have sufficiently diminished. However, the thermal period has a significant impact on repository conditions and lasts from hundreds to tens of thousands of years after waste package emplacement. Therefore, a computational study was performed to study seepage into drifts during the thermal period.

2. The Model

The NUFT code used in this study solves the partial differential equations for the flow and transport of air, water, and energy in a porous medium. The treatment of fractures uses the equivalent continuum model (ECM) which has been widely-used in previous studies, and is implemented in NUFT according to the method described in Nitao (1988). The ECM assumes equilibrium between the fractures and matrix and is adequate for flow under quasi-steady conditions. Future studies will investigate the use of the dual permeability option in NUFT in modeling seepage under highly transient percolation conditions.

2.1. Model Geometry and Mesh

A two-dimensional periodic drift-scale model was used with drift spacing of 28 m according to the "point loading" design for a 85 MTU/acre repository. The drift radius is 5.5 m in diameter (see Fig. 1) which assumes that the drift-wall ground supports are not present. Ground supports, if they remain intact, would affect seepage by directing water between them and the driftwall and, perhaps, some water would flow out of the joints between pre-cast support sections. Our model does not have backfill material (The reference design does not have backfill material). The reference design of the invert was not finalized at the time of the start of the study. Consequently, a gravel invert is used.

The model domain is 694 m tall and extends from the water table to the ground surface. A grid with square elements 0.3 m wide and tall placed around the drift (Fig. 1) is nested into a coarser main grid. The fine grid is required to resolve the flow which can strongly affect seepage, especially around the crown of the drift, and because the resolution of the grid has to be smaller than the correlation length of the heterogeneous hydrological properties. Also, the circular geometry of the drift has to be adequately resolved because of its potential influence on flow streamlines around the drift.

2.2. Hydrologic Parameters

Although the ECM treats the fractured rock as a single continuum, hydrological properties for the fracture and matrix can have different heterogeneous spatial distributions which can be generated using a stochastic spectral method (Nitao, 1997). The fracture K_f and matrix K_m permeabilities are generated stochastically according to a log-normal random field possessing a gaussian power spectrum with isotropic correlation length equal to 1 m. The fracture porosity ϕ_f, fracture van Genuchten α_f parameter, and matrix van Genuchten α_m parameter are related to the permeabilities by the following assumed scaling laws,

$$\phi_f \sim \sqrt{K_f} \tag{2.1}$$

$$\alpha_f \sim \sqrt{K_f}, \tag{2.2}$$

$$\alpha_m \sim \sqrt{K_m}. \tag{2.3}$$

The bulk permeability K_b is approximately equal to $\phi_f K_f$ so that we have

$$K_b \sim K_f^{3/2}. \tag{2.4}$$

The portion of the domain in the fine grid around the drift has spatially heterogeneous properties. The remainder of the domain has layered units with spatially uniform properties within each layer.

The stochastic generation algorithm requires mean values for the hydrological parameters within the spatially heterogeneous subdomain around the drift. Two sets of values were used for this subdomain and for the other geological units within the model domain: the 1997 TSPA-VA "base case" and the set from Klavetter and Peters (1986).

The TSw35 unit contains the emplacement drift in our model if the TSPA-VA data set is used. The parameter values for this unit are given in Table 2.1.

Table 2.1 1997 TSPA-VA Hydrological Properties for TSw35 Unit

fracture permeability K_f	4.19e-9 m^2
fracture porosity ϕ_f	3.29e-4
fracture residual saturation S_{rf}	0.01
van Genuchten α_f	1.10e-4 1/Pa
van Genuchten n_f	1.969
matrix permeability K_m	1.55e-17 m^2
matrix porosity ϕ_m	0.115
matrix residual saturation S_{rm}	0.08
van Genuchten α_m	3.31e-6 1/Pa
van Genuchten n_m	1.297
bulk dry thermal conductivity K_H	2.1 W/m-C
bulk wet thermal conductivity K_H	2.1 W/m-C
grain heat capacity	9.0e2 J/kg
grain density	2.54e3 kg/m^3

For the Klavetter and Peters property set, the repository is in the TSw1 unit. Its parameter values are given in Table 2.2. The fracture properties are equivalent to a 100 micron aperture parallel plate fracture with properties of a well-sorted sand.

Table 2.2 Hydrological Properties of TSw1 based on Klavetter and Peters (1986)

fracture permeability K_f	8.33e-10 m^2
fracture porosity ϕ_f	3.330e-4
fracture residual saturation S_{rf}	0.04
van Genuchten α_f	1.315e-3 1/Pa
van Genuchten n_f	4.23
matrix permeability K_m	1.9e-18 m^2
matrix porosity ϕ_m	0.110
matrix residual saturation S_{rm}	0.08
van Genuchten α_m	5.8e-7 1/Pa
van Genuchten n_m	1.798
bulk dry thermal conductivity K_H	1.5 W/m-C
bulk wet thermal conductivity K_H	2.13 W/m-C
grain heat capacity	9.0e2 J/kg
grain density	2.54e3 kg/m^3

2.3. Thermal Radiation

Because of the fine spatial discretization around the drift, there a large number of elements on the surface of the drift wall, resulting in numerous radiation connections from drift wall to drift wall elements, drift wall to waste package elements, and drift to invert elements. These connections, which can number on the order of at least several thousand, are tedious to generate by hand, especially for three dimensional problems.

A computer program was developed to create these connections for two-dimensional and three-dimensional problems. It automatically checks whether the line-of-sight between elements does not intersect a waste package before a connection is made. The program also takes into account radiation reflections from optional axial and/or transverse symmetry planes. Currently, only a single reflection stage is implemented. Because reflections can increase the number of connections, the program goes back and removes any connections between the same pairs of elements after adding together their radiation coefficients. In some cases, especially in three dimensional problems, the large number of radiation connections can be prohibitive. The program loops through each connection and drops those whose contribution to the total viewfactor is much smaller than a user specified tolerance. Also, the user has the option to drop any connections whose angle from the surface normal is larger than a given threshold. Because of these and other approximations, the viewfactor of the waste package may not total to unity. The program has the option to adjust the coefficients of the connections so that the waste package view factor is normalized to unity.

The program can treat not only a single waste package but multiple waste packages. It also generates the specification in the NUFT input file for the location of the various material types in the model, such as the location of the drift, waste package, and invert with respect to the grid indices.

A GUI interface to the program is planned to improve its usability. The program is meant to be used for fine-grid models and is not appropriate at this time for coarse-grid models because the size of the exposed surface area of the radiating elements have to be small compared to the distance between elements.

2.4. Heat Load

The heat load is a composite of three types of waste packages from the 85 MTU/acre CSNF design: 21PWR (5.436 MTU), 21PWR (8.148 MTU), and 21 PWR (9.051 MTU).

2.5. Boundary Conditions and Initial Conditions

A constant uniform flux is applied to the top of the model. The sides of the model are no-flow boundaries. The bottom is fixed at constant saturation, pressure, dissolved air mass fraction, and temperature. Gas phase is not allowed to flow from the water table.

The initial conditions are obtained by running the model at the specified percolation flux with no drift and no heat until steady state conditions are reached.

3. Simulation Results

Simulations were first run using the TSPA-VA property set under heat and no-heat conditions. Figures 2 and 3 show the net liquid phase seepage flux into the drift as a function of time for the cases with homogeneous and heterogeneous rock, respectively. The negative flux is due to condensation of water vapor into the drift wall. As the air in the drift is heated, water vapor condenses onto the cooler drift wall and is imbibed by capillarity. The condensation stops as temperature of the drift wall reaches the boiling point of water. The imbibition flux is higher for the heterogeneous case.

Figures 4 and 5 show the same corresponding cases using the Klavetter and Peter data set. For this case there is a net positive flux of liquid phase into the drift due to the same phenomena as before, except that the rock cannot imbibe the water fast enough, so it must drain into the drift. The liquid saturation of the rock using the Klavetter and Peters properties is quite high at 5 mm/y as compared to the TSPA-VA properties; and, therefore, its capacity to imbibe condensate is much less. In Figure 7 note that the seepage stops after the temperature at the ceiling reaches the local boiling point of water (96°). Also, note that in the heterogeneous case there is an erratic fluctuation in seepage flux and that some seepage occurs after the drift wall temperature drops below the boiling point.

The bulk liquid saturation shown in Figure 6 demonstrates the non-uniform dryout of the rock in the heterogeneous Klavetter and Peters case at 100 years. Figure 7 is the liquid saturation inside the drift at 3 years. It graphically reveals the liquid water seeping into the drift from the drift ceiling. The water evaporates before it reaches the hot waste package and invert floor because we have to impose an artificially small liquid relative permeability at small saturations (the function $kr_\ell = S_\ell^4$ was used) in the drift in order to eliminate the small time constant associated with the falling water; otherwise, the resulting small time steps in our numerical solution algorithm would have made the simulation impractical. (Note that where there is seepage the model uses the upstream relative permeability which is that of the rock and not the relative permeability of the drift.) The small drift relative permeability slows the velocity of the water and allows time for the heat in the drift to evaporate it while it is still falling. In actuality, we expect the water to reach the hot waste package or floor and boil-off upon contact.

Figure 8 compares the case of a "line load" configuration which corresponds to preserving the areal mass loading while shortening the axial spacing between waste packages by a 0.60 factor. The pre-boiling time period of condensate drainage is predicted by our simulations to last less than a year. Note that the benefit of the line load is that there is no post-boiling condensate drainage. Another benefit, which is not simulated in our two dimensional model, is the resulting more uniform heat load which will reduce the likelihood of water vapor moving along the drift from hotter to cooler regions where it can condense.

A parameter study was performed to make a zero-th order estimate of the effects of possible alteration of fracture properties by geomechanical or geochemical processes. We modified the region out to a single drift radius (2.75 m) from the drift wall. Uniform hydrological properties were used with parameter values equal to that of the surrounding rock mass but with fracture permeability decreased by a factor of 0.01 and fracture porosity decreased by 0.1. A second case was run with fracture permeability increased by 100 and porosity by 10. As shown in Figure 9, decreased fracture permeability around the drift reduces the likelihood of seepage from the rock. (Water condensing onto the ceiling surface might also drip onto the waste package, but our model does not include the details of this phenomena.) Note that the case with increased fracture permeability has a higher seepage flux, especially during the post-boiling period.

4. Summary

We have developed the capability to model the seepage of water from a heterogeneous formation under nonisothermal conditions using the NUFT code. A program has been written to automatically generate, for two and three-dimensional models, the radiation connections between the drift wall to drift wall, drift wall to waste package, and drift wall to invert elements. This capability includes the connections due to virtual reflections about symmetry planes.

Before the temperature at the drift wall reaches the boiling point of water, radioactive decay heat from waste packages can alter seepage conditions by giving rise to seepage of condensed water in the rock. This phenomena can occur for both boiling and sub-boiling repository designs. The seepage fluxes during this period are significantly higher than percolation fluxes and can range on the order of 10's to 100's of millimeters per year. The likelihood of such fluxes depends strongly on the hydrological properties and conditions of the surrounding rock mass. For example, at a percolation flux of 5 mm/y, such fluxes were observed with Klavetter and Peters (1986) properties, but not with 1997 TSPA-VA properties.

The duration of this condensation period is relatively short. Seepage stops after the rock reaches boiling temperature. In some cases water may also come back into the drift after the temperature at the drift wall comes back down to below-boiling conditions. Calculations show that the length of the condensate drainage period is reduced from approximately 4 years for the point load design to approximately 1 year for the "line-load" configuration. In exchange for the shorter seepage period, the amount of seepage flux is roughly doubled over that of the point load design. Another advantage of the line load compared to the point load is the absence of seepage during the post-boiling period.

A parameter study was performed to make a simple estimate of the effects of rock mass alteration by geomechanical or geochemical processes. Decreased fracturing out to within one drift radius from the drift wall was found to decrease condensation seepage, whereas increased fracturing led to increased condensation seepage especially during the post-boiling period.

References

Buscheck, T.A., J.J. Nitao, and L.D. Ramspott, Localized Dryout: An Approach for Managing the Thermal-Hydrological Effects of Decay Heat at Yucca Mountain, Proceedings of the Materials Research Society XIX International Basis for Nuclear Waste Management, Boston, Mass, Nov 27-Dec 1, 1995.

Klavetter, E.A., and R.R. Peters, Estimation of Hydrologic Properties of An Unsaturated, Fractured Rock Mass," SAND84-2642, Sandia National Laboratories, 1986.

Nitao, J.J., Numerical Modeling of the Thermal and Hydrological Environment around a Nuclear Waste Package using the Equivalent Continuum Approximation: Horizontal Emplacement, Lawrence Livermore National Laboratory Report UCID-21444, 1988.

Nitao, J.J., and T.A. Buscheck, Discrete-Fracture Modeling of Thermal-Hydrological Processes at Yucca Mountain and the LLNL G-Tunnel Field Test, Proceedings of the Materials Research Society XIX International Basis for Nuclear Waste Management, Boston, Mass, Nov 27-Dec 1, 1995.

Nitao, J.J., Preliminary Bounds for the Drift-Scale Distribution of Percolation and Seepage at the Repository Level under Pre-Emplacement Conditions, Deliverable No. SPLB1M4, 1997.

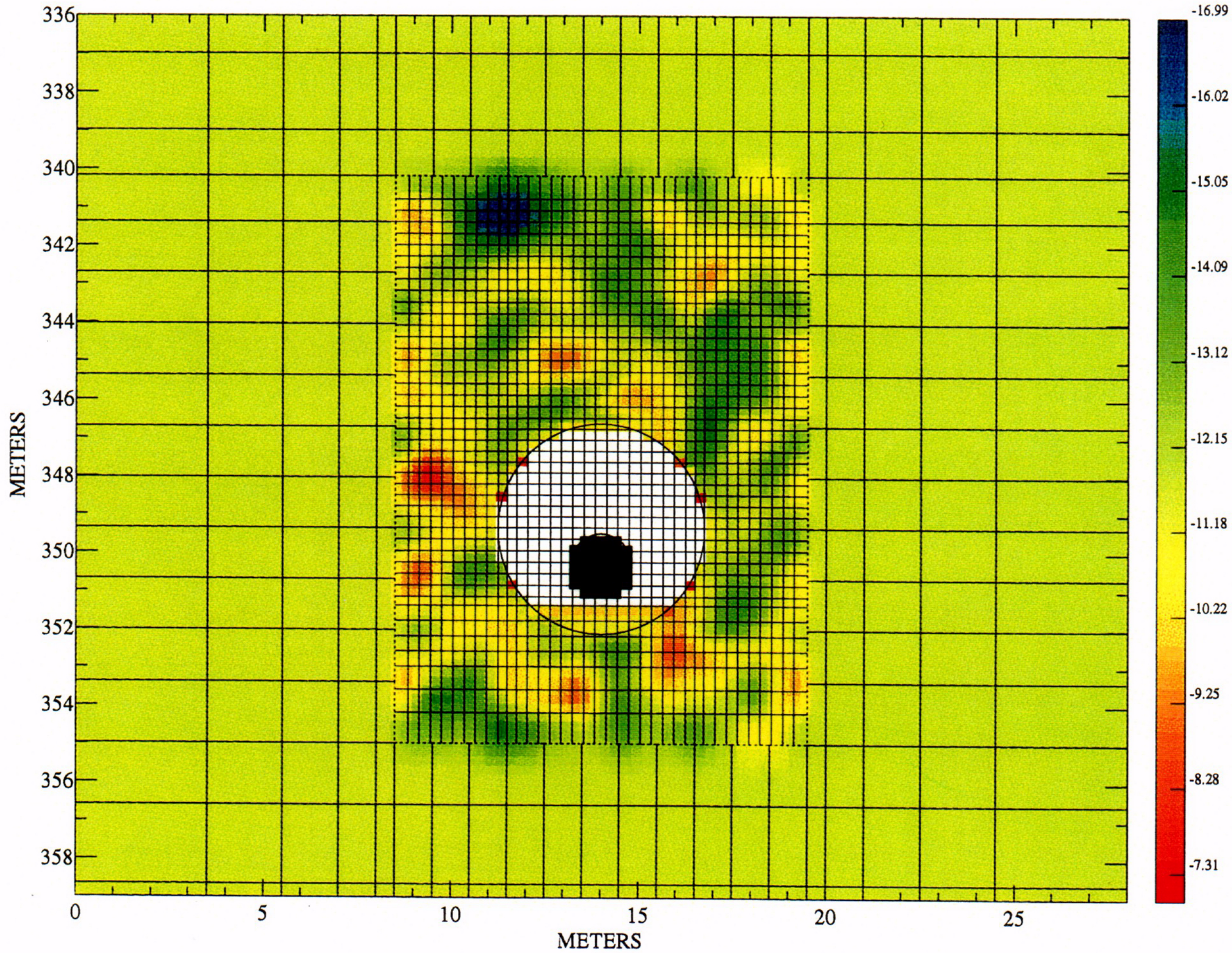

Figure 1. Close-up of the nested grid and the log10 bulk permeability field around the drift.

C01

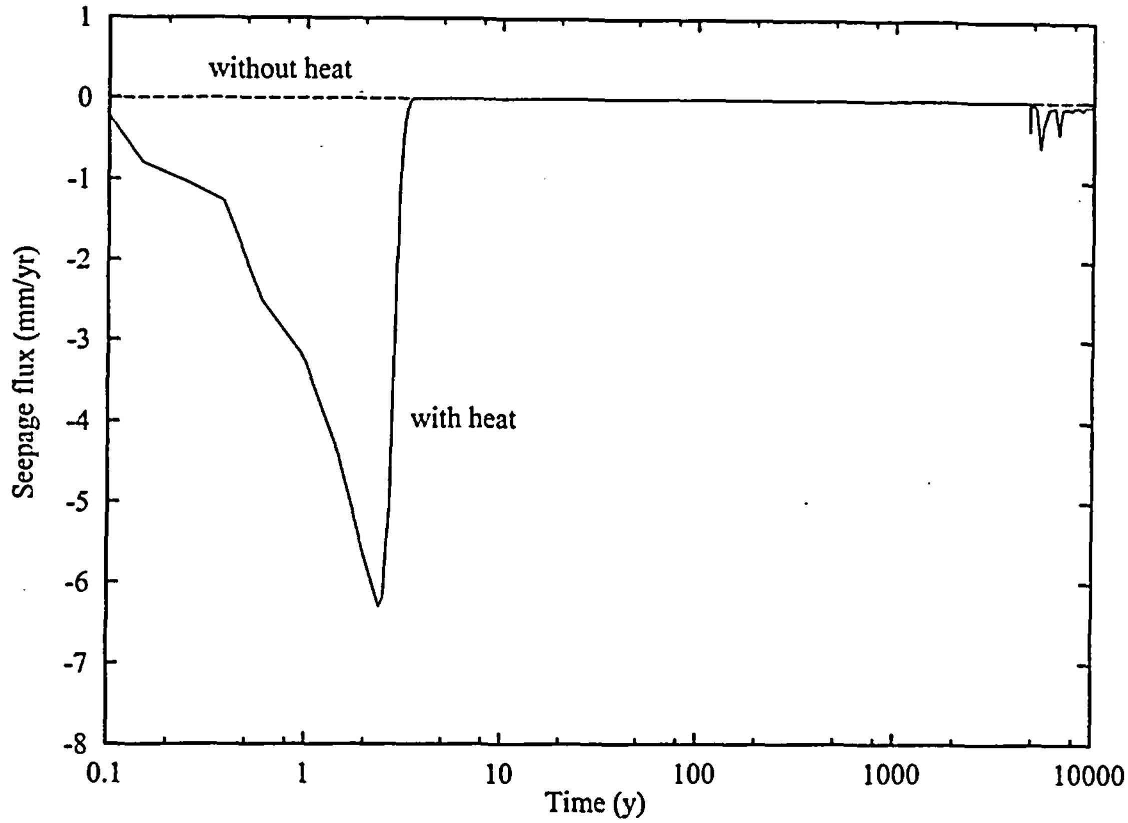

Figure 2. Seepage flux into the drift for the homogeneous, 5 mm/y case under point loading with the TSPA-VA property set.

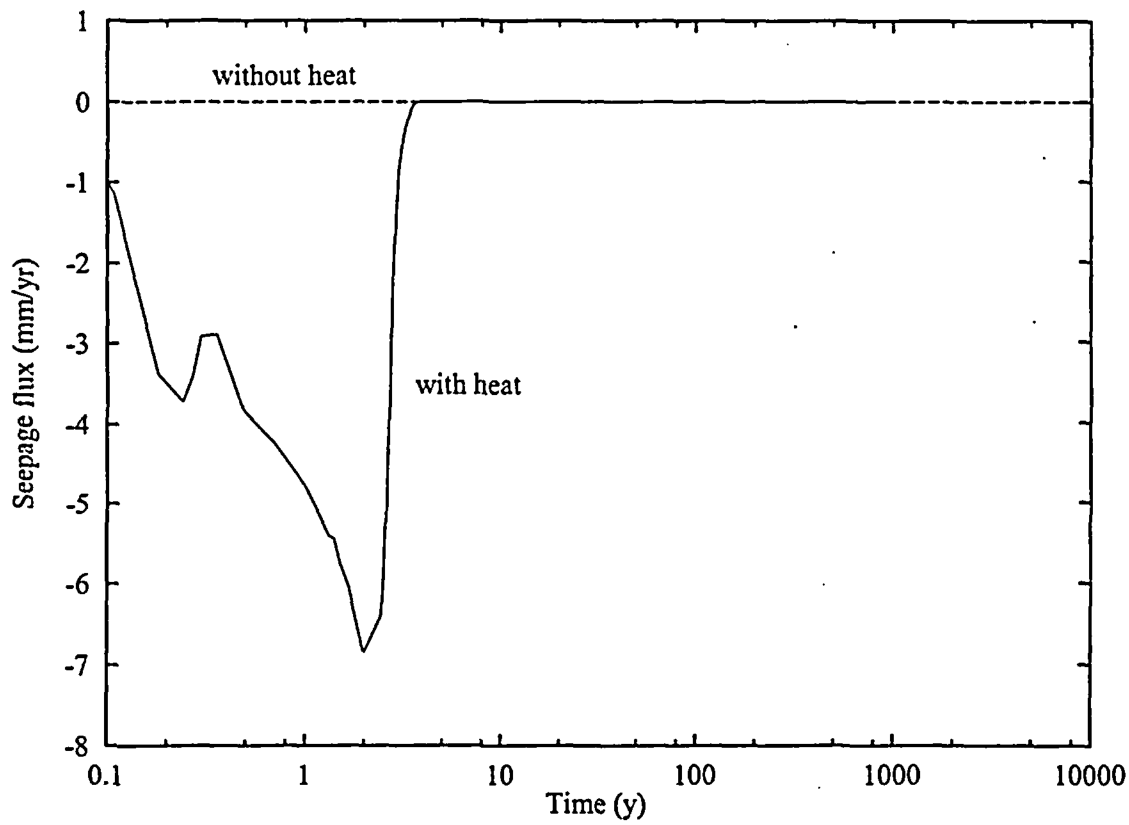

Figure 3. Seepage flux into the drift for the heterogeneous, 5 mm/y case under point loading with the TSPA-VA property set.

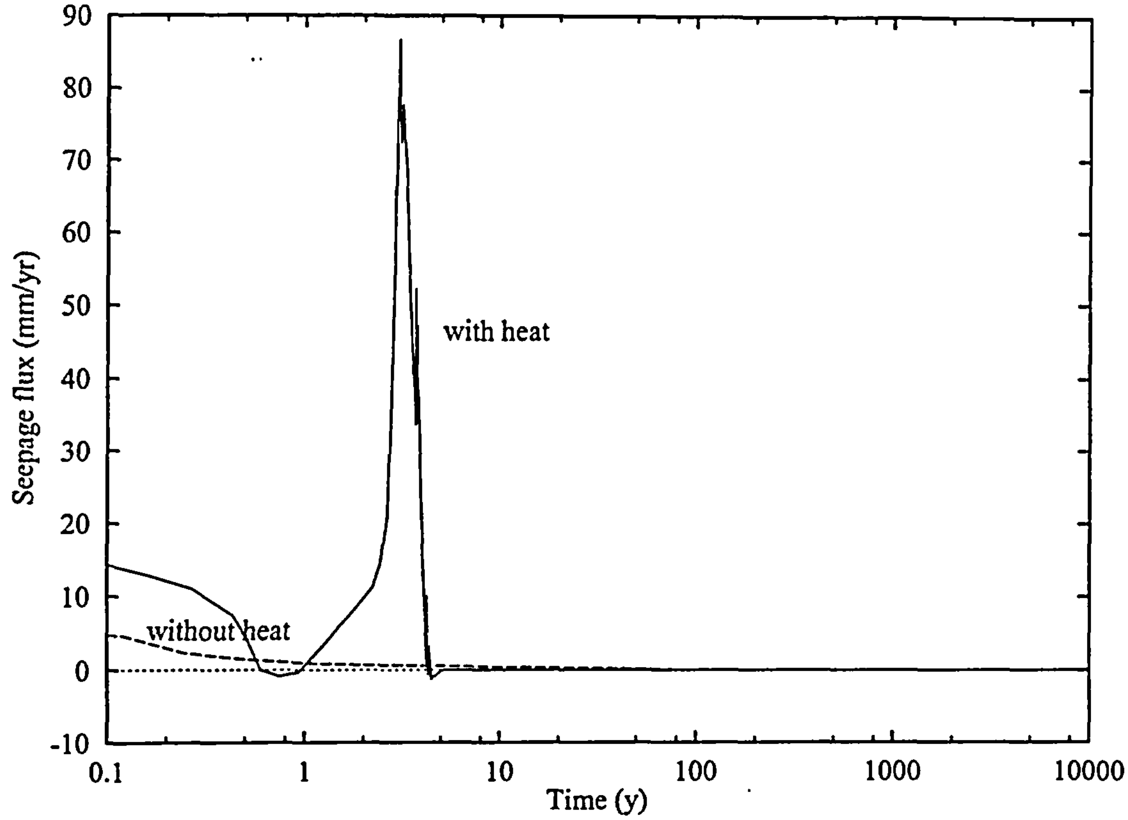

Figure 4. Seepage flux into the drift for the homogeneous, 5 mm/y case under point loading with the Klavetter and Peters property set.

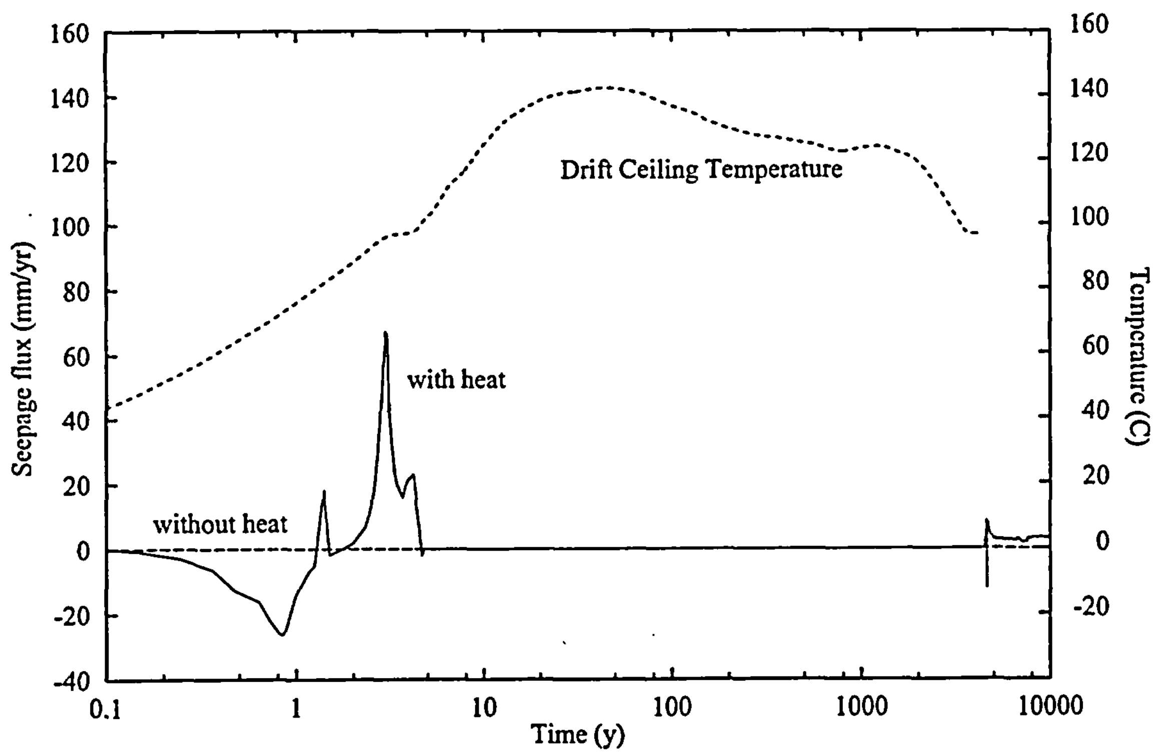

Figure 5. Seepage flux into the drift for the heterogeneous, 5 mm/y case under point loading with the Klavetter and Peters property set.

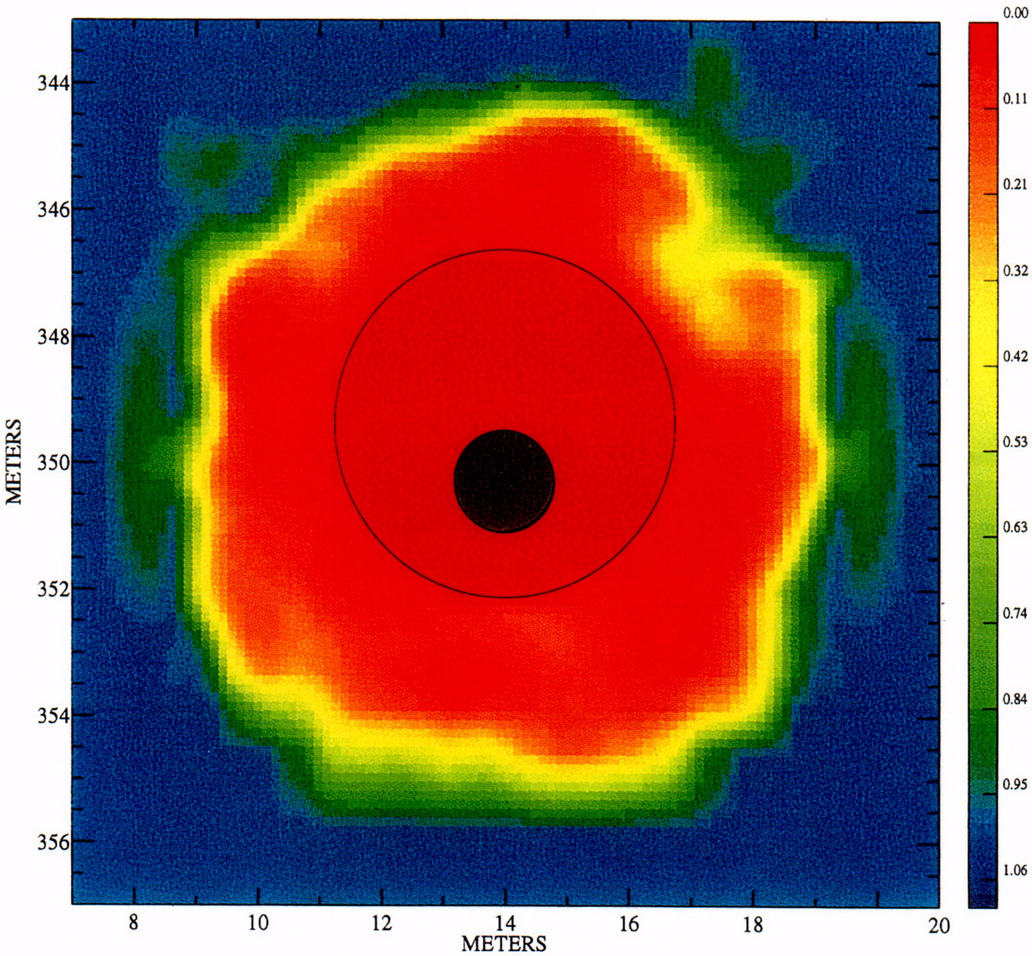

Figure 2. Bulk liquid saturation at 10 years for 5 mm/y with the Klavetter and Peters data set with spatially heterogeneous hydrological properties.

C02

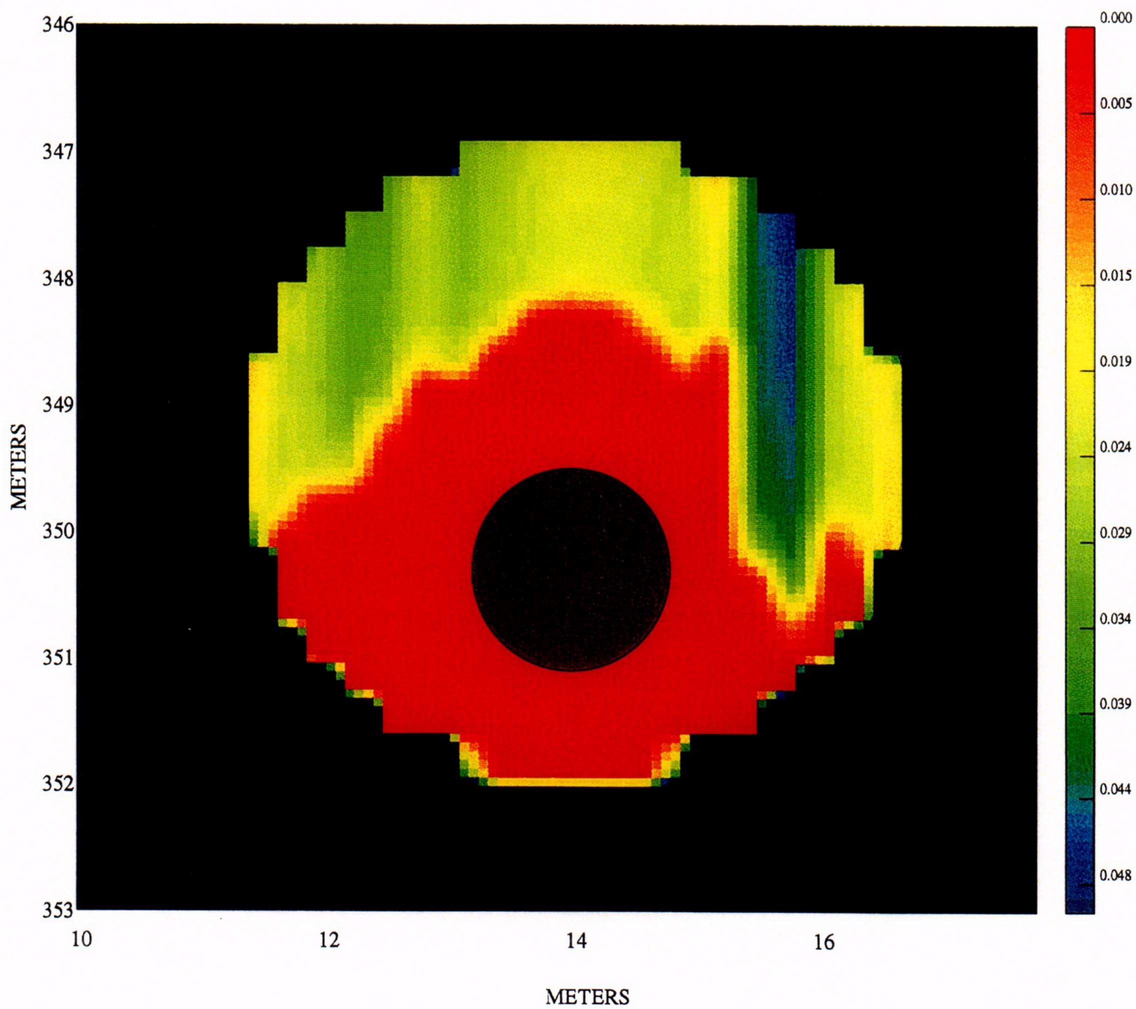

Figure 7. Liquid saturation in the drift at 3 years for 5 mm/y percolation flux using the Klavetter and Peters property set with heterogeneous variation. Seepage in the drift is caused by condensation of water vapor onto and within the cooler drift wall at early times. Seepage ceases after temperatures in the rock reach the boiling point. Evaporation of water is overestimated in the model because of artificially low relative permeability in the drift to facilitate numerical computation.

C03

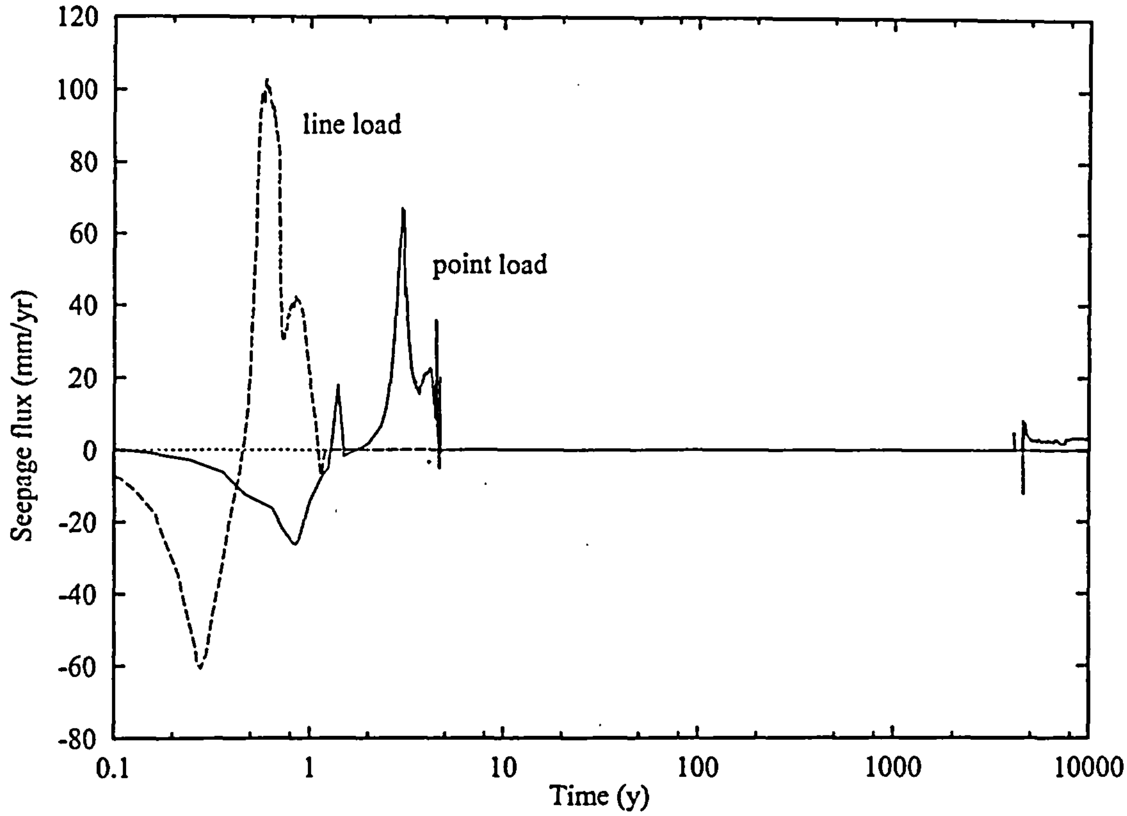

Figure 8. Seepage flux into the drift for the heterogeneous 5 mm/y case with the Klavetter and Peters property set -- comparison between line and point loading.

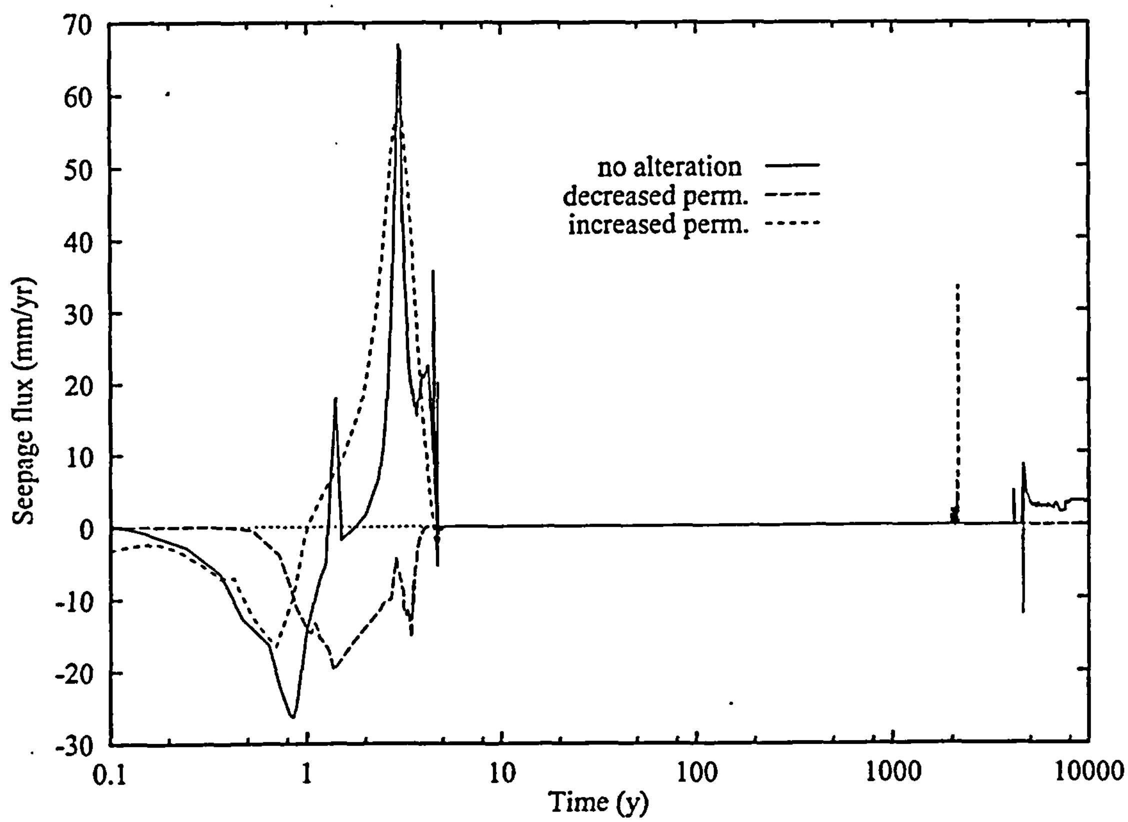

Figure 9. Seepage flux into the drift for the heterogeneous 5 mm/y case under point loading with the Klavetter and Peters property set -- effect of altering the degree of fracturing around the drift.

DRAFT DISCLAIMER